A Rigorous Modal Analysis of H-Plane Waveguide T-Junction Loaded with a Partial-Height Post for Wide-Band Applications

Ke-Li Wu, *Senior Member, IEEE,* and Haiyin Wang

***Abstract*—A rigorous modal analysis (MA) for the H-plane waveguide T-junction loaded with a partial-height conducting post is presented in this paper. The analysis is based on the classical resonator mode-matching technique for waveguide junction problems and a novel concept called *extended eigenmode functions*. The new concept can be used for constructing eigenmode functions of a complex resonator region as long as the modal solution for a subproblem is available. Particularly for the T-junction problem, the modal solution for the two-port in-line waveguide loaded with the post is used. The proposed MA has been extensively verified by a finite-element method software package. Excellent agreement can be observed. Numerical results obtained by the analysis reveal that by adjusting the dimension of the loading post, the usable band width of the T-junction for constructing a diplexer can be significantly expanded. Since the generalized scattering matrix is obtained, the proposed analysis can be integrated with other available waveguide key building-block models for system analysis.**

***Index Terms*—Mode-matching method, waveguide components, waveguide junctions.**

I. Introduction

An H-PLANE waveguide T-junction is a fundamental circuit element in rectangular waveguide circuits for dividing signal to different paths. Among various applications of the standard H-plane T-junction, the feeding structures for slotted waveguide antenna arrays [1], the manifold multiplexers with narrow-band channel filters [2], [3], and some narrow-band diplexers [4] are most noticeable. With the increasing demands of high data-rate transmission for wireless communications, the wide-band microwave and millimeter-wave communication systems have attracted considerable attention. For instance, some front-end diplexers for the local multipoint distribution system (LMDS) at 28 GHz may require about 5% bandwidth to cover transmitting and receiving bands. Therefore, research for wide-band microwave devices and circuits become more and more important today.

A good theoretical foundation has been laid for designing wide-band diplexers using symmetric three-port junctions [5], in which it has been shown that, if the T-junction satisfies certain criteria, channel filters, and, consequently, the diplexer constructed by the filters will have maximum bandwidths. One of the criteria to be satisfied is that $S'_{22}(f) \approx 0$, $S'_{12}(f) \approx 0$, $S'_{23}(f) \approx 0$ over the frequency band of interest, where port 2 is the common port and the prime indicates the derivative with respect to frequency f. More recently, the criteria have been used in designing wide-band Ka-band H-plane diplexers, where a modified H-plane T-junction with an inductive window was used [6].

Although it has been well known for a long time that, in practice, the usable bandwidth of a diplexer using an H-plane T-junction can be expanded by introducing a tuning screw at the center of the T-junction, a thorough theoretical investigation to reveal the mystery has not been seen by the authors thus far in spite of the fact that some relevant work have been done to this end, e.g., Galerkin's method of moments was adopted for obtaining the dominant-mode scattering parameters for a simplified situation: a full-height post-loaded H-plane T-junction [1]. In regard to this, a rigorous analysis of an H-plane T-junction loaded with a partial-height conducting post would be significantly important since it represents a more general case. Furthermore, to integrate the T-junction modal analysis (MA) module with other waveguide key MA modules, having a generalized scattering matrix (GSM) would be the most desirable feature for design engineers because the GSM takes into account the mutual couplings among all the higher order modes.

In this paper, an MA model is developed for a rigorous analysis of an H-plane T-junction loaded with a partial-height conducting post, as shown in Fig. 1. A new concept, called *extended eigenmode functions*, for constructing mode functions of a complex resonator region, is proposed and used. It will be demonstrated that, with the aid of the new concept, an MA for a complex problem can be facilitated by the modal solution of a simpler subproblem. It can be perceived that the concept can be easily used to solve an H-plane T-junction with other kinds of loading as long as the modal solution for the subproblem, in which the middle arm of the T-junction is shorted, is available. To illustrate the basic principle of the MA, only the structure of a partial-height conducting post is considered in this paper. The developed model has been verified by comparing the results obtained by the proposed model with those of a commercial finite-element-method software. To provide a sort of reference to engineering designs, the performances of the H-plane T-junctions with some typical post loading are also given for Ku- and Ka-band applications. The performances disclose that the dimensions of a partial-height conducting post in the T-junction, particularly the height, play a critical role in expanding the usable bandwidth.

Manuscript received May 10, 2000; revised July 31, 2000.

K.-L. Wu is with the Department of Electronic Engineering, The Chinese University of Hong Kong, Shatin, Hong Kong.

H. Wang is with the Department of Electrical and Computer Engineering, McMaster University, Hamilton, ON, Canada L8S 4K1.

Publisher Item Identifier S 0018-9480(01)03304-X.

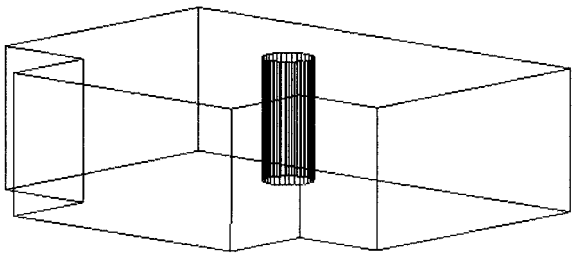

Fig. 1. H-plane waveguide T-junction loaded with a partial-height conducting post.

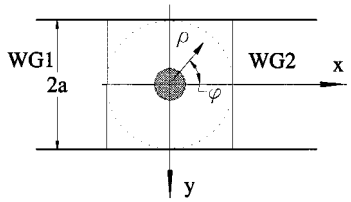

Fig. 2. Top view of the rectangular waveguide loaded with a post and the subregions for the MA.

II. MA

A. Two-Port In-Line Post-Loaded Waveguide Discontinuity

It is assumed that the GSM of a post-loaded waveguide discontinuity can be solved using an MA [7], [8], where an artificial cylindrical boundary of radius a is introduced to facilitate the field matching between the region using a cylindrical coordinate system and the rectangular waveguide regions. For the completeness of analysis, a brief outline of the MA using orthogonal expansion is given here.

To apply the orthogonal expansion method, the two-port waveguide discontinuity is divided into waveguide regions WG1 and WG2, and a post interaction region bounded by the artificial cylindrical boundary of radius a, as shown in Fig. 2. The fields in the post interaction region are expressed by a linear combination of the cylindrical mode functions. The fields in waveguide regions WG1 and WG2 are expressed as

$$\begin{Bmatrix} \vec{E}_t^{\mathrm{WG1}} \\ \vec{E}_t^{\mathrm{WG2}} \end{Bmatrix} = \sum_q \left\{ \begin{bmatrix} A_q^{1,h} e^{-\gamma_q^h x} + B_q^{1,h} e^{\gamma_q^h x} \\ B_q^{2,h} e^{-\gamma_q^h x} + A_q^{2,h} e^{\gamma_q^h x} \end{bmatrix} \right\} \vec{e}_{t,q}^{\,h} + \sum_q \left\{ \begin{bmatrix} A_q^{1,e} e^{-\gamma_q^e x} + B_q^{1,e} e^{\gamma_q^e x} \\ B_q^{2,e} e^{-\gamma_q^e x} + A_q^{2,e} e^{\gamma_q^e x} \end{bmatrix} \right\} \vec{e}_{t,q}^{\,e} \quad (1a)$$

$$\begin{Bmatrix} \vec{H}_t^{\mathrm{WG1}} \\ \vec{H}_t^{\mathrm{WG2}} \end{Bmatrix} = \sum_q \left\{ \begin{bmatrix} A_q^{1,h} e^{-\gamma_q^h x} - B_q^{1,h} e^{\gamma_q^h x} \\ B_q^{2,h} e^{-\gamma_q^h x} - A_q^{2,h} e^{\gamma_q^h x} \end{bmatrix} \right\} \vec{h}_{t,q}^{\,h} + \sum_q \left\{ \begin{bmatrix} A_q^{1,e} e^{-\gamma_q^e x} - B_q^{1,e} e^{\gamma_q^e x} \\ B_q^{2,e} e^{-\gamma_q^e x} - A_q^{2,e} e^{\gamma_q^e x} \end{bmatrix} \right\} \vec{h}_{t,q}^{\,e} \quad (1b)$$

for transverse-field components, as designated by the subscript t, and

$$\begin{Bmatrix} E_x^{\mathrm{WG1}} \\ E_x^{\mathrm{WG2}} \end{Bmatrix} = \sum_q \left\{ \begin{bmatrix} A_q^{1,h} e^{-\gamma_q^h x} - B_q^{1,h} e^{\gamma_q^h x} \\ B_q^{2,h} e^{-\gamma_q^h x} - A_q^{2,h} e^{\gamma_q^h x} \end{bmatrix} \right\} e_{x,q}^{e} \quad (1c)$$

$$\begin{Bmatrix} H_x^{\mathrm{WG1}} \\ H_x^{\mathrm{WG2}} \end{Bmatrix} = \sum_q \left\{ \begin{bmatrix} A_q^{1,h} e^{-\gamma_q^h x} + B_q^{1,h} e^{\gamma_q^h x} \\ B_q^{2,h} e^{-\gamma_q^h x} + A_q^{2,h} e^{\gamma_q^h x} \end{bmatrix} \right\} h_{x,q}^{h} \quad (1d)$$

for longitudinal components, as designated by the subscript x, where As and Bs are the coefficients corresponding to the incident and reflected waves at each waveguide port and the superscripts h and e correspond to TE and TM modes, respectively.

The boundary conditions on all the natural boundaries are enforced to be satisfied by taking cross inner products of the electric-field continuity equations with the magnetic field of the eigenmodes at the exterior region of the boundary and to the magnetic-field continuity equations with the electric field of the eigenmodes at the interior region of the boundary. The fields in the waveguide regions are matched to those in the cylindrical region by applying the electric- and magnetic-field boundary conditions on the artificial boundary via taking appropriate cross inner products of the field continuity equations with magnetic- and electric-field eigenmodes of the interior region of the boundary, respectively.

The above-mentioned boundary condition matching process leads to the GSM for a rectangular waveguide loaded with a post structure

$$\begin{Bmatrix} B^1 \\ B^2 \end{Bmatrix} = \begin{bmatrix} S_{11} & S_{12} \\ S_{21} & S_{22} \end{bmatrix} \begin{Bmatrix} A^1 \\ A^2 \end{Bmatrix} \quad (2)$$

where A^i and B^i are the coefficient vectors containing the coefficients of both TE and TM modes in WG1 and WG2, for $i = 1$ and 2, respectively.

B. Problem of the Post-Loaded Waveguide T-Junction

Considering a waveguide T-junction loaded with a partial-height conducting post in the center, in light of the resonator eigenmode technique for solving junction types of problems [9], we can divide the T-junction into four regions: waveguide 1 (WG1), waveguide 2 (WG2), waveguide 3 (WG3), and resonator region (R)—the center square with the post bounded by S1, S2, and S3 and a conducting wall, as shown in Fig. 3. The tangential electromagnetic fields in WG1, WG2, and WG3 at waveguide apertures S1, S2, and S3, respectively, can be expressed in terms of unknown mode coefficients $\{A^{Wi}\}$ for the incident waves and $\{B^{Wi}\}$ for the reflected waves as

$$\begin{Bmatrix} \vec{E}_t^{\mathrm{WG1}} \\ \vec{E}_t^{\mathrm{WG2}} \\ \vec{E}_t^{\mathrm{WG3}} \end{Bmatrix} = \sum_q \left\{ \begin{bmatrix} [A_q^{W1,h} + B_q^{W1,h}] \\ [A_q^{W2,h} + B_q^{W2,h}] \\ [A_q^{W3,h} + B_q^{W3,h}] \end{bmatrix} \right\} \vec{e}_{t,q}^{\,h} + \sum_q \left\{ \begin{bmatrix} [A_q^{W1,e} + B_q^{W1,e}] \\ [A_q^{W2,e} + B_q^{W2,e}] \\ [A_q^{W3,e} + B_q^{W3,e}] \end{bmatrix} \right\} \vec{e}_{t,q}^{\,e} \quad (3a)$$

$$\begin{Bmatrix} \vec{H}_t^{\mathrm{WG1}} \\ \vec{H}_t^{\mathrm{WG2}} \\ \vec{H}_t^{\mathrm{WG3}} \end{Bmatrix} = \sum_q \left\{ \begin{bmatrix} [A_q^{W1,h} - B_q^{W1,h}] \\ [B_q^{W2,h} - A_q^{W2,h}] \\ [B_q^{W3,h} - A_q^{W3,h}] \end{bmatrix} \right\} Y_q^h \begin{Bmatrix} \hat{x} \\ \hat{y} \\ \hat{x} \end{Bmatrix} \times \vec{e}_{t,q}^{\,h} + \sum_q \left\{ \begin{bmatrix} [A_q^{W1,e} - B_q^{W1,e}] \\ [B_q^{W2,e} - A_q^{W2,e}] \\ [B_q^{W3,e} - A_q^{W3,e}] \end{bmatrix} \right\} Y_q^e \begin{Bmatrix} \hat{x} \\ \hat{y} \\ \hat{x} \end{Bmatrix} \times \vec{e}_{t,q}^{\,e} \quad (3b)$$

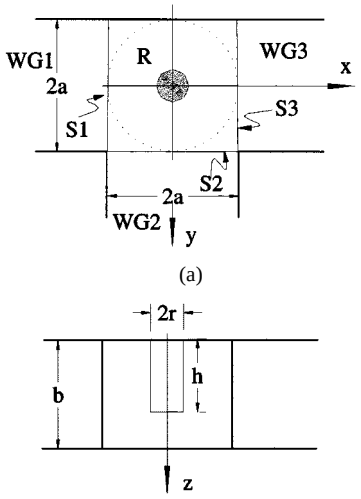

Fig. 3. Top and front views of the waveguide T-junction loaded with a partial-height conducting post.

where $i = 1, 2,$ and 3, $\overline{e}^{h}_{t,q}$ and $\overline{e}^{e}_{t,q}$ are the qth transverse-mode functions in the rectangular waveguide of TE and TM modes, respectively, and Y^h_q and Y^e_q are the corresponding wave admittances.

By an application of a superposition principle, the total fields in region R can be superposed by the field solutions satisfying boundary conditions illustrated by Fig. 4(a)—case 1, Fig. 4(b)—case 2, and Fig. 4(c)—case 3, respectively, such that

$$\vec{E}^R = \sum_q C^1_q \vec{\Phi}^1_q + \sum_q C^2_q \vec{\Phi}^2_q + \sum_q C^3_q \vec{\Phi}^3_q \tag{4a}$$

$$\vec{H}^R = \sum_q C^1_q \vec{\Psi}^1_q + \sum_q C^2_q \vec{\Psi}^2_q + \sum_q C^3_q \vec{\Psi}^3_q \tag{4b}$$

where $\vec{\Phi}^i_q$ and $\vec{\Psi}^i_q$ are the qth *distinct* solutions of the electric and magnetic fields, respectively, with respect to case i, $i = 1, 2,$ and 3.

C. Extended Eigenmode Functions

A question then arises as how to determine the qth distinct solution as the qth eigenmode function in the resonator region to be used in (4a) and (4b). Intuitively, it can be found out that the required eigenmode functions can be constructed by the solution of the two-port in-line waveguide discontinuity loaded with the post. Due to the rotation symmetry of the three boundary value problems shown in Fig. 4, only one of them, say, the problem shown in Fig. 4(a), needs to be solved for constructing the eigenmodes. If the fields in WG1, WG2, and WG3 are expanded by nh terms of TE modes and ne terms of TM modes after truncating an infinite long eigenmode expansion, we need to have $nh + ne$ pairs of independent ($\vec{\Phi}^1$, $\vec{\Psi}^1$) mode functions.

Suppose we have the GSM of the waveguide discontinuity loaded with the post, as shown in Fig. 2, by shifting the reference plane of port 2 from the center of the post to $x = a$, we can find

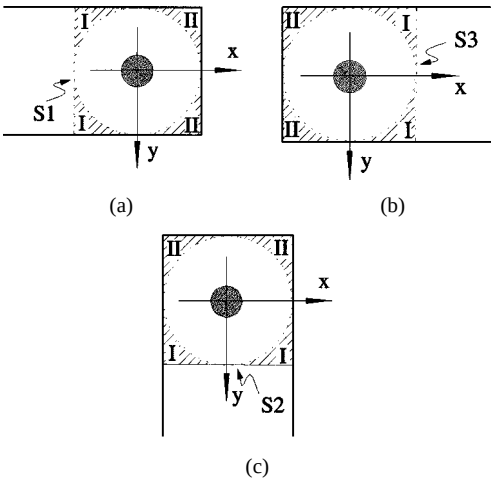

Fig. 4. Boundary conditions for the extended eigenmode functions for the post-loaded waveguide T-junction.

the GSM of the one-port problem with port 2 short circuited, as shown in Fig. 4(a). It reads

$$\{B^1\} = \Big\{[S_{11}] + [S_{12}][e^{-\gamma a}]\Big([I] + [e^{-\gamma a}][S_{22}][e^{-\gamma a}]\Big)^{-1} \cdot [e^{-\gamma a}][S_{21}]\Big\}\{A^1\} \tag{5a}$$

or

$$\{B^1\} = [S_M]\{A^1\} \tag{5b}$$

where $[e^{-\gamma a}]$ is a diagonal matrix with its elements equal to either $e^{-\gamma^h_q a}$ or $e^{-\gamma^e_q a}$, depending on the type of the corresponding mode, and $[I]$ is the unitary matrix. The following relations are needed for determining the coefficients of the modes in the short-circuited waveguide WG2:

$$\{A^2\} = -[e^{-\gamma a}]\Big([I] + [e^{-\gamma a}][S_{22}][e^{-\gamma a}]\Big)^{-1} \cdot [e^{-\gamma a}][S_{21}]\{A^1\} \tag{6}$$

and

$$[e^{-2\gamma a}]\{B^2\} = -\{A^2\}. \tag{7}$$

To construct $nh+ne$ independent eigenmode functions, $nh+ne$ independent incident waves are launched to excite the system shown in Fig. 4(a). Mathematically, the $nh+ne$ incident waves can be expressed by $nh + ne$ independent vectors of $\{A^1\}$ as

$$\{A^1_1\} = \begin{Bmatrix} 1 \\ 0 \\ 0 \\ 0 \\ \vdots \\ 0 \end{Bmatrix}$$

$$\{A^1_2\} = \begin{Bmatrix} 0 \\ 1 \\ 0 \\ 0 \\ \vdots \\ 0 \end{Bmatrix}$$

$$\{A_3^1\} = \begin{Bmatrix} 0 \\ 0 \\ 1 \\ 0 \\ \vdots \\ 0 \end{Bmatrix} \cdots$$

$$\{A_N^1\} = \begin{Bmatrix} 0 \\ 0 \\ 0 \\ 0 \\ \vdots \\ 1 \end{Bmatrix} \tag{8}$$

where $N = nh + ne$.

Since $[S_M]$ is a known system function, we can obtain N responses $\{B_1^1\}, \{B_2^1\}, \ldots, \{B_N^1\}$ corresponding to the incident vectors such that

$$\{B_i^1\} = [S_M]\{A_i^1\}. \tag{9}$$

Consequently, we can obtain $\{A_i^2\}$ and $\{B_i^2\}$, $i = 1, 2, \ldots, N$, from (6) and (7). In the above coefficient vectors, the first nh elements correspond to TE modes and the rest of ne elements correspond to TM modes. That is, for the ith independent excitation, there are

$$\{A_i^j\}^T = \{A_i^{j,h}, A_i^{j,e}\}^T \quad \text{and} \quad \{B_i^j\}^T = \{B_i^{j,h}, B_i^{j,e}\}^T, \quad j = 1, 2. \tag{10}$$

It can be observed that, for matching the tangential fields at each waveguide port, we only need to know the field in the four shaded corner regions, namely regions I and II, as shown in Fig. 4. Fortunately, the field expressions in the regions, as given in (1a)–(1d), only involve rectangular coordinate system. Therefore, once the matrix $[S_M]$ is obtained, no coordinate conversions are needed for solving the T-junction problem.

With the coefficients of the incident and the reflected waves of $nh + ne$ independent solutions determined above, the eigenmode functions required for the shaded regions in R can be constructed. For example, the qth eigenmode in subregions I and II is given by

$$\begin{aligned}\vec{\Phi}_q^{1\binom{I}{II}}(x, y, z) &= \sum_k^{nh} \left\{ \begin{pmatrix} A_{q,k}^{1,h} \\ B_{q,k}^{2,h} \end{pmatrix} e^{-\gamma_k^h x} + \begin{pmatrix} B_{q,k}^{1,h} \\ A_{q,k}^{2,h} \end{pmatrix} e^{\gamma_k^h x} \right\} \vec{e}_{t,k}^{\,h}(y, z) \\ &+ \sum_k^{ne} \left\{ \begin{pmatrix} A_{q,k}^{1,e} \\ B_{q,k}^{2,e} \end{pmatrix} e^{-\gamma_k^e x} + \begin{pmatrix} B_{q,k}^{1,e} \\ A_{q,k}^{2,e} \end{pmatrix} e^{\gamma_k^e x} \right\} \vec{e}_{t,k}^{\,e}(y, z) \\ &+ \sum_k^{ne} \left\{ \begin{pmatrix} A_{q,k}^{1,e} \\ B_{q,k}^{2,e} \end{pmatrix} e^{-\gamma_k^e x} - \begin{pmatrix} B_{q,k}^{1,e} \\ A_{q,k}^{2,e} \end{pmatrix} e^{\gamma_k^e x} \right\} e_{x,k}^{e}(y, z)\hat{x}\end{aligned} \tag{11a}$$

$$\begin{aligned}\vec{\Psi}_q^{1\binom{I}{II}}(x, y, z) &= \sum_k^{ne} \left\{ \begin{pmatrix} A_{q,k}^{1,e} \\ B_{q,k}^{2,e} \end{pmatrix} e^{-\gamma_k^e x} - \begin{pmatrix} B_{q,k}^{1,e} \\ A_{q,k}^{2,e} \end{pmatrix} e^{\gamma_k^e x} \right\} \vec{h}_{t,k}^{\,e}(y, z) \\ &+ \sum_k^{nh} \left\{ \begin{pmatrix} A_{q,k}^{1,h} \\ B_{q,k}^{2,h} \end{pmatrix} e^{-\gamma_k^h x} - \begin{pmatrix} B_{q,k}^{1,h} \\ A_{q,k}^{2,h} \end{pmatrix} e^{\gamma_k^h x} \right\} \vec{h}_{t,k}^{\,h}(y, z) \\ &+ \sum_k^{nh} \left\{ \begin{pmatrix} A_{q,k}^{1,h} \\ B_{q,k}^{2,h} \end{pmatrix} e^{-\gamma_k^h x} + \begin{pmatrix} B_{q,k}^{1,h} \\ A_{q,k}^{2,h} \end{pmatrix} e^{\gamma_k^h x} \right\} h_{x,k}^{h}(y, z)\hat{x}\end{aligned} \tag{11b}$$

where the subscript t and x refer to the transverse and the longitudinal components with respect to the x-axis, respectively. The eigenmode functions of $\vec{\Phi}_q^{2\binom{I}{II}}(x, y, z)$ and $\vec{\Psi}_q^{2\binom{I}{II}}(x, y, z)$ can be derived from (11a) and (11b) by changing x to $-y$ and y to x. To obtain $\vec{\Phi}_q^{3\binom{I}{II}}(x, y, z)$ and $\vec{\Psi}_q^{3\binom{I}{II}}(x, y, z)$ from (11a) and (11b), we only need to change x to $(x + 2a)$ to ensure the consistency of the field polarization reference at ports 1 and 3.

Due to the fact that the eigenmode functions obtained above are extensions of the modal solution of a canonical problem, the eigenmode functions derived in such a scheme are called *extended eigenmode functions*.

D. Matching of Field Continuities

Both the tangential electric and magnetic fields of region R at apertures S1, S2, and S3 are enforced to be matched with those of WG1, WG2, and WG3, respectively, by taking inner products of the matched tangential fields with appropriate mode functions in the corresponding waveguide. For example, the continuity of the tangential electric field at S1

$$\vec{E}_{\tan \text{ to S1}}^{R}\Big|_{x=-a} = \vec{E}_t^{\text{WG1}}\Big|_{x=-a} \tag{12a}$$

or

$$\begin{aligned}\sum_k^{nh+ne} C_k^1 \vec{\Phi}_{t,k}^{1I}(-a, y, z) &= \sum_q \left(A_q^{W1,h} + B_q^{W1,h}\right) \vec{e}_{t,q}^{\,h} \\ &+ \sum_q \left(A_q^{W1,e} + B_q^{W1,e}\right) \vec{e}_{t,q}^{\,e}\end{aligned} \tag{12b}$$

will be enforced by taking inner product of the above equation with $\vec{e}_{t,p}^{\,h}$ and $\vec{e}_{t,p}^{\,e}$ over S1, which leads to

$$\sum_k^{nh+ne} C_k^1 Q_{kp}^{1,h} = A_p^{W1,h} + B_p^{W1,h}, \qquad p = 1, 2, \ldots, nh \tag{13a}$$

$$\sum_k^{nh+ne} C_k^1 Q_{kp}^{1,e} = A_p^{W1,e} + B_p^{W1,e}, \qquad p = 1, 2, \ldots, ne \tag{13b}$$

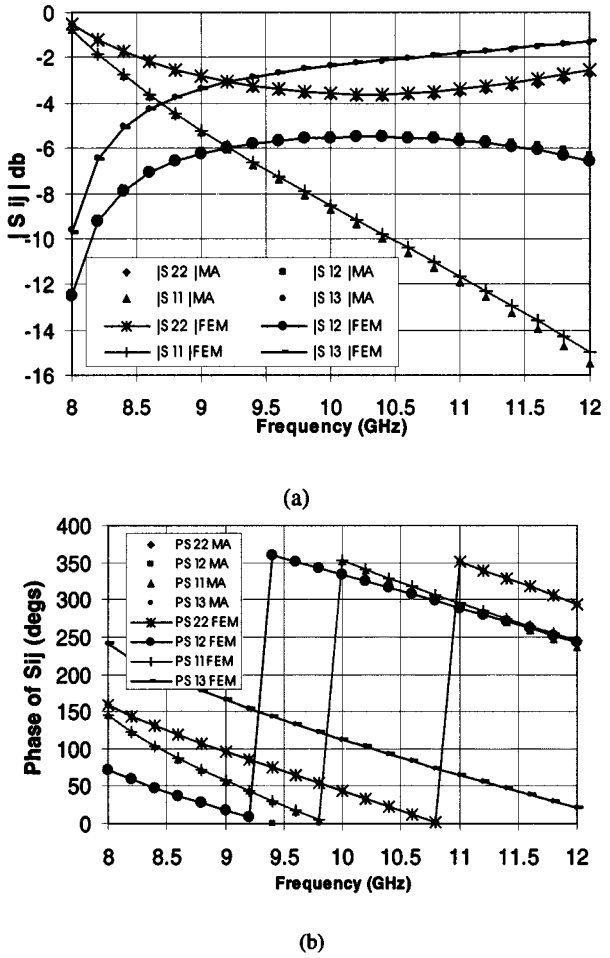

Fig. 5. WR75 (0.75 in × 0.375 in) rectangular waveguide T-junction loaded with a partial-height conducting post with radius of 0.05 in and a post height of 0.1 in. Comparison between the scattering parameters obtained by the proposed MA and by the FEM software. (a) Magnitude of the S-parameters. (b) Phase of the S-parameters.

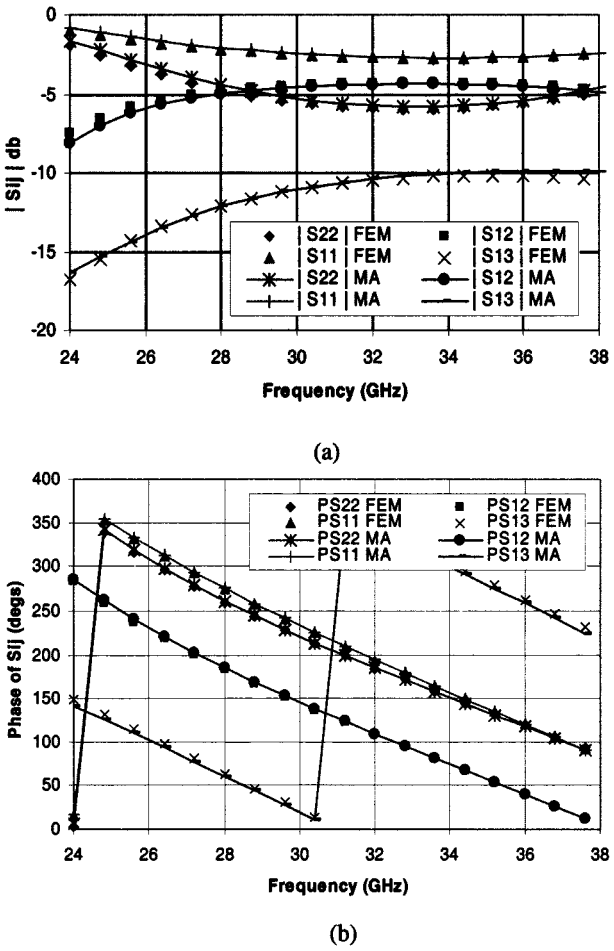

Fig. 6. WR28 (0.28 in × 0.14 in) rectangular waveguide T-junction loaded with a partial-height conducting post with radius of 0.025 in and post height of 0.12 in. Comparison between the scattering parameters obtained by the proposed MA and FEM software. (a) Magnitude of the S-parameters. (b) Phase of the S-parameters.

where the orthogonal and normal properties of the mode functions have been employed, and the coefficients

$$Q_{kp}^{1,\binom{h}{e}} = \left\langle \vec{\Phi}_{t,k}^{1I},\, \vec{e}_{t,p}^{\binom{h}{e}} \right\rangle = \begin{pmatrix} A_{k,p}^{1,h} \\ A_{k,p}^{1,e} \end{pmatrix} e^{\gamma_k^h a} + \begin{pmatrix} B_{k,p}^{1,h} \\ B_{k,p}^{1,e} \end{pmatrix} e^{-\gamma_k^h a}. \tag{14}$$

In the above process, the fact that the tangential components of $\vec{\Phi}_{t,k}^{2}$ and $\vec{\Phi}_{t,k}^{3}$ at port aperture S1 equal to zero has been used in (12a) and (12b). As a result, only the field quantities associated with $\vec{\Phi}_{t,k}^{1}$ are considered in (12a) and (12b). By the same token, the tangential electric fields at S2 and S3 can be matched, leading to the electric-field matching matrix equation

$$\underbrace{\begin{bmatrix} Q^{1,h} & 0 & 0 \\ Q^{1,e} & 0 & 0 \\ 0 & Q^{2,h} & 0 \\ 0 & Q^{2,e} & 0 \\ 0 & 0 & Q^{3,h} \\ 0 & 0 & Q^{3,e} \end{bmatrix}}_{[Q]} \begin{Bmatrix} C^1 \\ C^2 \\ C^3 \end{Bmatrix} = \begin{Bmatrix} A^{W1,h} + B^{W1,h} \\ A^{W1,e} + B^{W1,e} \\ A^{W2,h} + B^{W2,h} \\ A^{W2,e} + B^{W2,e} \\ A^{W3,h} + B^{W3,h} \\ A^{W3,e} + B^{W3,e} \end{Bmatrix}. \tag{15}$$

It can be easily found that $Q^{1,h} = Q^{2,h} = Q^{3,h}$ and $Q^{1,e} = Q^{2,e} = Q^{3,e}$.

The magnetic-field matching process at each of the port apertures is more complicated than that of the electric field due to the nonzero tangential magnetic field of extended eigenmode functions at the short-circuited ports. For example, the following continuity of the tangential magnetic field at S1:

$$\begin{aligned} &\sum_{k}^{nh+ne} C_k^1 \vec{\Psi}_{t,k}^{1I}(-a, y, z) \\ &\quad + \sum_{k}^{nh+ne} C_k^2 \begin{pmatrix} \vec{\Psi}_{t,k}^{1II}(-a, y, z), -a \le y \le 0 \\ \vec{\Psi}_{t,k}^{1I}(-a, y, z), 0 \le y \le -a \end{pmatrix} \\ &\quad + \sum_{k}^{nh+ne} C_k^3 \vec{\Psi}_{t,k}^{3II}(-a, y, z) \\ &= \sum_{q}^{nh} \left(A_q^{W1,h} - B_q^{W1,h} \right) Y_q^h \left(\hat{x} \times \vec{e}_{t,q}^{\,h} \right) \\ &\quad + \sum_{q}^{ne} \left(A_q^{W1,e} - B_q^{W1,e} \right) Y_q^e \left(\hat{x} \times \vec{e}_{t,q}^{\,e} \right) \end{aligned} \tag{16}$$

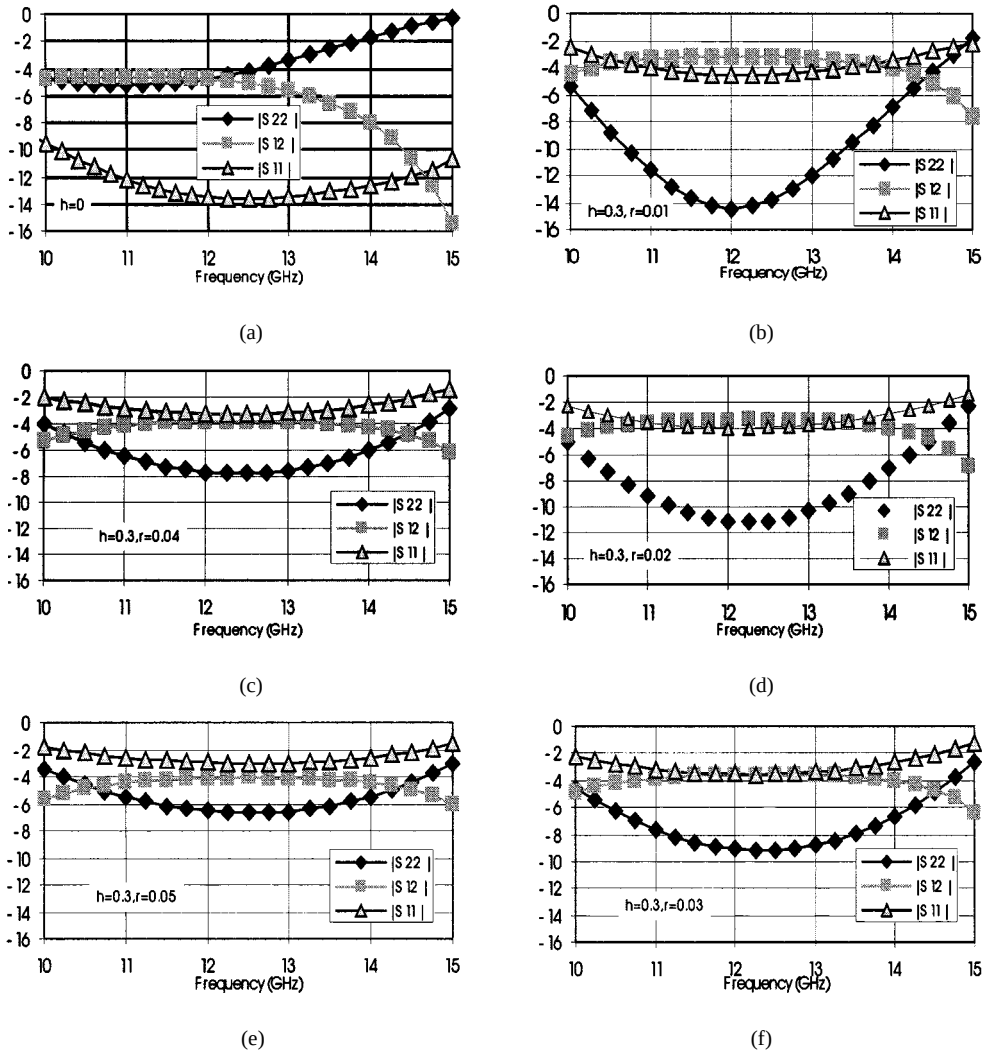

Fig. 7. Selected magnitude (in decibels) of S-parameters of the H-plane Ku-band WR75 waveguide T-junction loaded with a conducting post of varied radius (from 0.01 to 0.05 in) and 0.3-in post height.

will be satisfied by taking the inner product of (16) on both sides with $(\hat{x} \times \vec{e}^{\,h}_{t,p}(y, z))$, $p = 1, 2, \ldots, nh$ and $(\hat{x} \times \vec{e}^{\,e}_{t,p}(y, z))$, $p = 1, 2, \ldots, ne$. The procedure of the inner product leads to

$$\sum_{k}^{nh+ne} C_k^1 U_{kp}^{1,1h} + \sum_{k}^{nh+ne} C_k^2 U_{kp}^{2,1h} + \sum_{k}^{nh+ne} C_k^3 U_{kp}^{3,1h} = \left(A_p^{W1,h} - B_p^{W1,h}\right), \qquad p = 1, 2, \ldots, nh \tag{17a}$$

$$\sum_{k}^{nh+ne} C_k^1 U_{kp}^{1,1e} + \sum_{k}^{nh+ne} C_k^2 U_{kp}^{2,1e} + \sum_{k}^{nh+ne} C_k^3 U_{kp}^{3,1e} = \left(A_p^{W1,e} - B_p^{W1,e}\right), \qquad p = 1, 2, \ldots, ne \tag{17b}$$

where

$$U_{kp}^{1,1h} = \left\langle \vec{\Psi}_{t,k}^{1I}(-a, y, z), \left(\hat{x} \times \vec{e}^{\,h}_{t,p}(y, z)\right) \right\rangle \Big/ Y_p^h \tag{18a}$$

$$U_{kp}^{2,1h} = \left\langle \begin{pmatrix} \vec{\Psi}_{t,k}^{2II}(-a, y, z), -a \le y \le 0 \\ \vec{\Psi}_{t,k}^{2I}(-a, y, z), 0 \le y \le -a \end{pmatrix}, \left(\hat{x} \times \vec{e}^{\,h}_{t,p}(y, z)\right) \right\rangle \Big/ Y_p^h \tag{18b}$$

$$U_{kp}^{3,1h} = \left\langle \vec{\Psi}_{t,k}^{3II}(-a, y, z), \left(\hat{x} \times \vec{e}^{\,h}_{t,p}(y, z)\right) \right\rangle \Big/ Y_p^h \tag{18c}$$

$$U_{kp}^{1,1e} = \left\langle \vec{\Psi}_{t,k}^{1I}(-a, y, z), \left(\hat{x} \times \vec{e}^{\,e}_{t,p}(y, z)\right) \right\rangle \Big/ Y_p^e \tag{18d}$$

$$U_{kp}^{2,1e} = \left\langle \begin{pmatrix} \vec{\Psi}_{t,k}^{2II}(-a, y, z), -a \le y \le 0 \\ \vec{\Psi}_{t,k}^{2I}(-a, y, z), 0 \le y \le -a \end{pmatrix}, \left(\hat{x} \times \vec{e}^{\,e}_{t,p}(y, z)\right) \right\rangle \Big/ Y_p^e \tag{18e}$$

$$U_{kp}^{3,1e} = \left\langle \vec{\Psi}_{t,k}^{3II}(-a, y, z), \left(\hat{x} \times \vec{e}^{\,e}_{t,p}(y, z)\right) \right\rangle \Big/ Y_p^e. \tag{18f}$$

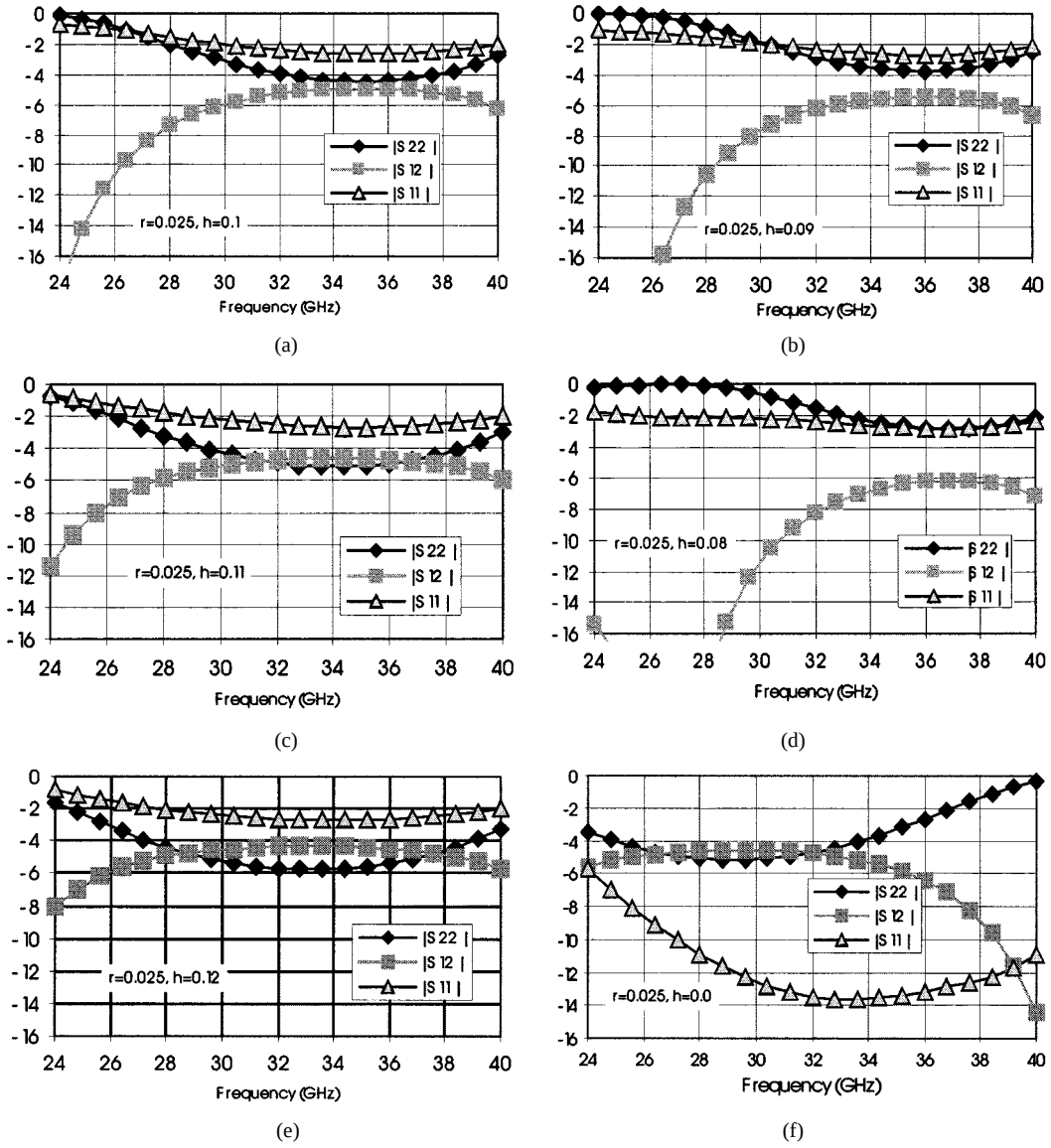

Fig. 8. Selected magnitude (in decibels) of S-parameters of the H-plane Ka-band WR28 waveguide T-junction loaded with a conducting post of 0.025-in radius and varied post height (from 0 to 0.12 in).

Applying the same procedure to S2 and S3 yields the magnetic-field matching matrix equation

$$\underbrace{\begin{bmatrix} U^{1,1h} & U^{2,1h} & U^{3,1h} \\ U^{1,1e} & U^{2,1e} & U^{3,1e} \\ -U^{1,2h} & -U^{2,2h} & -U^{3,2h} \\ -U^{1,2e} & -U^{2,2e} & -U^{3,2e} \\ -U^{1,3h} & -U^{2,3h} & -U^{3,3h} \\ -U^{1,3e} & -U^{2,3e} & -U^{3,3e} \end{bmatrix}}_{[U]} \begin{Bmatrix} C^1 \\ C^2 \\ C^3 \end{Bmatrix} = \begin{Bmatrix} A^{W1,h} - B^{W1,h} \\ A^{W1,e} - B^{W1,e} \\ A^{W2,h} - B^{W2,h} \\ A^{W2,e} - B^{W2,e} \\ A^{W3,h} - B^{W3,h} \\ A^{W3,e} - B^{W3,e} \end{Bmatrix}. \quad (19)$$

By eliminating the coefficient vector $\{C\}$ from (15) and (19), the desired GSM $[S]$ for the T-junction can be derived as

$$\begin{Bmatrix} B^{W1,h} \\ B^{W1,e} \\ B^{W2,h} \\ B^{W2,e} \\ B^{W3,h} \\ B^{W3,e} \end{Bmatrix} = \underbrace{\left[[I]+[U][Q]^{-1}\right]^{-1}\left[[I]-[U][Q]^{-1}\right]}_{[S]} \cdot \begin{Bmatrix} A^{W1,h} \\ A^{W1,e} \\ A^{W2,h} \\ A^{W2,e} \\ A^{W3,h} \\ A^{W3,e} \end{Bmatrix}. \quad (20)$$

The GSM can be used with the GSMs of other key-building blocks. A computer program was written using the proposed MA model. It has been found that when $nh = 42$, $ne = 36$, the scattering parameters seem to convergent very well.

III. Verification and Numerical Results

The verification of the proposed MA is done through the comparison of the results by the proposed model with those obtained by Ansoft's HFSS, a commercial finite-element method (FEM) software. In order to show the validity of the model to the applications in microwave and millimeter-wave communication frequency bands, the partial-height conducting post-loaded T-junction of WG75, the typical waveguide for Ku-band, and WG28, the typical waveguide for Ka-band, are elaborately studied. As shown in Figs. 5 and 6, excellent agreement can be observed between the MA results and the FEM results, both for the Ku-band T-junction and the Ka-band T-junction. It is worthwhile mentioning that, although the disparity of the computing time between the MA and FEM analysis is not very large (about 2 min with MA and 7 min with FEM for 20 frequency points), the feature of the MA of providing GSM prevails.

A set of selected S-parameters are presented in Fig. 7 for the Ku-band waveguide post-loaded T-junctions with a given height (0.3 in) and varied post radii. It reveals that, by changing the radius with an appropriate fixed height, the flatness of the S-parameters over a wide bandwidth and their magnitudes can be leveraged. As discussed in Section I, the flatness (diminution of the derivative with respect to frequency) is one of the important criteria for obtaining the maximum bandwidth. By further numerical investigations, it can be found that (not shown) the center of the frequency band with maximum flatness can be shifted by adjusting the height of the post. This set of curves can serve as a design reference for Ku-band diplexer if port 2 is chosen as the common port.

A similar set of curves are presented in Fig. 8 for the Ka-band post-loaded waveguide T-junctions. Instead of fixing the height, as in the case of Fig. 7, the radius is given in Fig. 8 as 0.025 in and height varies. It can be observed that a wide flat frequency band can also be obtained and shifted by tuning the height of the post. A similar wide flat frequency band response is also observed (not shown) with radius of 0.035 and height of 0.13 in. It means that, for a given radius of the post, people can likely find an optimal matching by changing the height of the post. Fig. 8 can be used as a reference for the design of Ka-band diplexers. It can be perceived that the optimal condition for designing a wide-band diplexer can be reached by adjusting both the radius and height of the loading post.

IV. Conclusions and Final Remarks

In this paper, a rigorous MA has been presented for the H-plane waveguide T-junction loaded with a post structure. The analysis is based on the classical resonator mode-matching scheme and the novel concept called the "extended eigenmode functions." The new concept can be used for solving many other complex canonical guided-wave problems as long as the subsystems for the resonator modes can be solved by an MA. For example, the post structure in the T-junction could be a dielectric post, and even a rectangular post structure, for which the modal solutions are known. The solution for the case of an off-centered post can also be obtained straightforwardly using the addition theorem of Bessel functions. Since the GSM of the T-junction is obtained, the proposed MA model can be cascaded with the developed MA key building blocks of other waveguide discontinuities for integrated system analysis and optimization design of wide-band applications.

The proposed model has been verified by a commercial software based on the FEM. Excellent agreement can be observed. To provide some reference for practical design, typical S-parameters for the Ku- and Ka-band rectangular waveguide T-junctions loaded with a conducting partial-height post are given. It can be expected that the proposed MA model will become a key-building block in the waveguide system design.

References

[1] J. Hirokawa, K. Sakruai, M. Ando, and N. Goto, "An analysis of a waveguide T-junction with an inductive post," *IEEE Trans. Microwave Theory Tech.*, vol. 39, pp. 563–566, Mar. 1991.

[2] J. D. Rhodes and R. Levy, "Design of general manifold multiplexers," *IEEE Trans. Microwave Theory Tech.*, vol. MTT-27, pp. 111–123, Feb. 1979.

[3] A. A. Kirilenko, S. L. Senkevich, V. I. Tkachenko, and B. G. Tysik, "Waveguide diplexer and multiplexer design," *IEEE Trans. Microwave Theory Tech.*, vol. 42, pp. 1393–1394, July 1994.

[4] J. Bornemann, S. Amari, and R. Vahldieck, "A combined mode-matching and coupled-integral-equations technique for the design of narrow-band H-plane waveguide diplexers," in *IEEE Int. Antennas Propagat. Symp.*, vol. 2, 1999, pp. 950–953.

[5] A. Morini and T. Rozzi, "Constraints to the optimum performance and bandwidth limitations of diplexers employing symmetric three-port junctions," *IEEE Trans. Microwave Theory Tech.*, vol. 44, pp. 242–248, Feb. 1996.

[6] Y. Rong, H.-W. Yao, K. A. Zaki, and T. G. Dolan, "Millimeter-wave Ka-band H-plane diplexers and multiplexers," *IEEE Trans. Microwave Theory Tech.*, vol. 47, pp. 2325–2330, Dec. 1999.

[7] H.-W. Yao, K. A. Zaki, A. E. Atia, and R. Hershtig, "Full wave modeling of conducting posts in rectangular waveguides and its applications to slot coupled combine filters," *IEEE Trans. Microwave Theory Tech.*, vol. 43, pp. 2824–2830, Dec. 1995.

[8] K.-L. Wu, R. R. Mansour, and H. Wang, "A full wave analysis of a conductor post insert reentrant coaxial resonator in rectangular waveguide combine filters," in *IEEE Int. Microwave Symp. Dig.*, June 1996, pp. 1639–1642.

[9] E. Kuhn, "A mode-matching method for solving field problems in waveguide and resonator circuits," *Arch. Elektr. Ubertragung*, vol. 27, pp. 511–518, 1973.

Ke-Li Wu (M'90–SM'96) received the B.S. and M.Eng. degrees from the Nanjing University of Science and Technology, Nanjing, China, in 1982 and 1985, respectively, and the Ph.D. degree from Laval University, Quebec, QC, Canada, in 1989.

From 1989 to 1993, he was with the Communications Research Laboratory, McMaster University, as a Research Engineering and Research Group Manager. In March 1993, he joined the Corporate Research and Development Division, ComDev International, where he had been a Principle Member of Technical Staff in charge of development of advanced electromagnetic design software for various microwave subsytems for communication satellite and wireless communications. He has been with the Department of Electronic Engineering, The Chinese University of Hong Kong, Shatin, Hong Kong, since October 1999, where he is currently an Associate Professor. He is also an Adjunct Associate Professor at McMaster University, Hamilton, ON, Canada. He has authored or co-authored numerous publications in the area of electromagnetic modeling and microwave and antenna engineering. He

contributed to *Finite Element and Finite Difference Methods in Electromagnetics Scattering* (Amsterdam, The Netherlands: Elsevier, 1990) and to *Computational Electromagnetics* (Amsterdam, The Netherlands: Elsevier, 1991). He holds one Canadian patent and one U.S. patent. His current research interests include all aspects of numerical methods in electromagnetics with emphasis on the analysis of guided wave structures, passive microwave circuits, and interconnections of integrated LTCC RF modules.

Dr. Wu was the recipient of the 1992 International Scientific Radio Union (URSI) Young Scientist Award, and the Industry Feedback Award presented by the Telecommunication Research Institute of Ontario in 1993, and ComDev's Achievement Award in 1998.

Haiyin Wang received the M.E.E.E. degree from Tsinghua University, Tsinghua, China, the M.E.E.E. degree from Memorial University of Newfoundland, St. John's, NF, Canada, and is currently working toward the Ph.D. degree at McMaster University, Hamilton, ON, Canada.

From 1983 to 1988, she was an Electrical Engineer with the Chinese Academy of Space Technology, Beijing, China, where she performed research on signal propagation between the ground station and the satellite and designing antennas for satellites and radars. Her current research interests include modeling and design of microwave devices and circuits.